J Electroceram (2011) 26:84–89
DOI 10.1007/s10832-011-9632-0

# Effects of rapid thermal annealing in different ambients on structural, electrical, and optical properties of ZnO thin films by sol-gel method

**Jia Li · Jin-Hua Huang · Yu-Long Zhang · Ye Yang · Wei-Jie Song · Xiao-Min Li**

Received: 29 November 2009 / Accepted: 24 January 2011 / Published online: 5 February 2011


**Abstract** We studied the effects of rapid thermal annealing in different ambients on the structural, electrical and optical properties of the sol-gel derived ZnO thin films. All the films after annealing showed highly degree of (002) oriented in the X-ray diffractometry (XRD) patterns. The effects of annealing ambients on electrical properties of the films were studied. Carrier concentration, resistivity and mobility were found to be distinguished after annealed in different ambients. The sample with the lowest resistivity of 0.095 Ω·cm and the largest mobility of 105.1 $cm^2/v{\cdot}s$ was achieved after annealing in vacuum. XPS results indicated that more oxygen vacancies existed on the ZnO surface when annealed in vacuum than that in $O_2$.

**Keywords** ZnO thin films · Sol-gel · Rapid thermal annealing

## 1 Introduction

ZnO is an attractive semiconductor with a wide direct band gap of 3.27 eV and a large exciton binding energy of 60 meV. It has many applications in various optical and electrical devices such as gas sensors, surface acoustic wave devices, light emitting diodes, transparent electrode of solar cells, and thin film transistor [1–3].

J. Li · J.-H. Huang · Y.-L. Zhang · Y. Yang · W.-J. Song (✉)
Ningbo Institute of Material Technology and Engineering,
Chinese Academy of Sciences,
Ningbo 315201, People's Republic of China
e-mail: weijiesong@nimte.ac.cn

J. Li · X.-M. Li
Shanghai Institute of Ceramics, Chinese Academy of Sciences,
Shanghai 200050, People's Republic of China

Since the physical properties of ZnO thin films are very important for the efficiency of ZnO based optoelectronic device, systematic studies of the structural, optical and electrical properties of ZnO thin films are necessary for achieving high-performance devices. Furthermore, it is reported that the physical properties of ZnO films strongly depend not only on growth techniques but also on post heat treatments such as annealing [4–9]. In this study, sol-gel technique is adopted to deposit ZnO thin films as it has distinct advantages such as easy and cheap operation, excellent compositional control, and homogeneity on the molecular level. Rapid thermal annealing (RTA) is often used in fabrication procedures since it can improve film quality and it has shorter cycle time and large flexibility compared to conventional furnace annealing (CFA) [10]. S. Y. Hu et al. studied on the effect of annealing temperature on the structure and optical properties of rf sputtered ZnO films by RTA [11]. The optimum RTA temperature was found to be at 600°C. Y. C. Lee et al. deposited ZnO thin films on Si substrate following RTA with different annealing time. The PL spectrum revealed a significant improvement in the UV luminescence of ZnO films following RTA for 1 min [12]. X. Q. Wei et al. reported structure and defects analysis of ZnO thin films deposited by PLD method and annealed in different ambients [13]. However, detailed information about electrical properties such as resistivity, carrier concentration and mobility were not given.

According to the previous work we had done, the effect of post-annealing temperature on structural and optical properties of ZnO thin films was investigated with the annealing temperatures increase from 450 to 800°C. The result showed that ZnO thin film annealed at 750°C demonstrated the best structural properties while further increase the temperature showed little improvement. In this work, we deposited ZnO thin films and annealed them in

different ambients by RTA at 750°C. The aim is to investigate the relationships between the annealing ambients and properties of the ZnO thin films in detail and to get the optimal structural and optoelectrical properties for versatile use.

## 2 Experimental

The ZnO thin films were fabricated using a sol-gel technique. Zinc acetate dihydrate ($Zn(CH_3COO)_2{\bullet}H_2O$) was used as a precursor material. Monoethanolamine (MEA) and 2-methoxyethanol were used as stabilizer and solvent, respectively. Zinc acetate dihydrate was first dissolved in a mixture of 2-methoxyethanol and MEA solution at room temperature. The molar ratio of MEA to zinc acetate ($Zn(CH_3COO)_2$) was maintained at 1.0 and the final concentration of precursor solution was kept as 1 M. The solution was stirred for 3 h to yield a clear and homogeneous solution. The solution was very stable, no notable change was found even after 1 month. Quartz glass was chosen as substrate. Before using, all the substrates were cleaned and degreased ultrasonically by ethanol and acetone for 10 min each. The solution was dropped onto quartz glass substrates with a rotating speed of 3,000 rpm for 30 s. After spin coating, the films were dried at 300°C for 10 min over a hot plate to evaporate the solvent and remove organic residuals. The procedure from coating to drying was repeated seven times. The films were then put into rapid annealing furnace and annealed at 750°C for 5 min. The thickness of the ZnO films in this study was about 100 nm as determined by SEM cross section. To investigate the effects of post-thermal annealing ambient on the structure, electrical optical constants of the as-prepared ZnO films, the films were annealed in different ambients. One sample was annealed in atmosphere pressure. One sample was annealed in vacuum with the pressure of 3 Pa. The others were annealed in $N_2$ and $O_2$ ambient, respectively. Flow rate of both nitrogen and oxygen is 1.5 L/min in atmosphere pressure.

XRD analysis for phase identification of as-prepared ZnO thin films was performed using a Burker AXS D8 advance diffractometer with Cu Kα radiation in the 2θ angles ranging from 20° to 80°. The morphologies of the products were observed by a Hitachi S-4800 field emission scanning electron microscope (FESEM). The resistivity was measured using a Pro4 resistivity system (Model Pro4-4000). Carrier concentration and mobility were measured and calculated by Hall measurement system (Quantum Design, PPMS-9). X-ray photoelectron spectroscopy (XPS, AXIS UTLTRADLD, Japan) was used to characterize the surface composition and chemical state of the products using Al Kα radiation. Optical transmittance measurements were recorded on a LAMBDA 950 UV-Visible spectrophotometer in the range of 200–1,000 nm.

## 3 Results and discussion

Figure 1 shows XRD spectra of as-grown ZnO and ZnO thin films annealed at 750°C in vacuum, nitrogen, oxygen gas and atmosphere ambients, respectively. The peaks identified comparing with JCPDS files for wurtzite type of ZnO. The as-grown ZnO film had only a small peak which indicated weak crystallization. After post-thermal annealing in RTA, the intensity of the diffraction peak of ZnO (002) strongly increased and the peak width was narrowed. The observation of dominant (002) peaks at ~34.4° indicated that the films were grown with a preferred c-axis orientation normal to the substrates.

In order to determine the degree of preferred orientation, the volume fraction $\alpha_{(002)}$ of c-axis-oriented grains in the ZnO films was defined as

$$\alpha_{(002)}(\%) = I_{(002)} / \left[ I_{(100)} + I_{(002)} + I_{(101)} \right]$$

Where $I_{(002)}$, $I_{(100)}$ and $I_{(101)}$ were the measured intensity of the (002), (100) and (101) diffraction peak for the ZnO thin films [14]. The $\alpha_{(002)}$ values for the annealed films were summarized in Table 1. It is shown that ZnO thin films annealed in atm and $O_2$ were highly c-axis oriented with $\alpha_{(002)}$ values 97.9% and 97.8%, respectively. After annealing in $N_2$, the degree of c-axis orientation decreased to 93.9% and it reached the minimum value when annealed in vacuum. This implied that the crystal quality was better for ZnO thin films annealed in abundant oxygen environment.

Since (002) peak was the most prominent growth orientation, we had calculated the full width at half maximum (FWHM) of this peak and calculated the grain

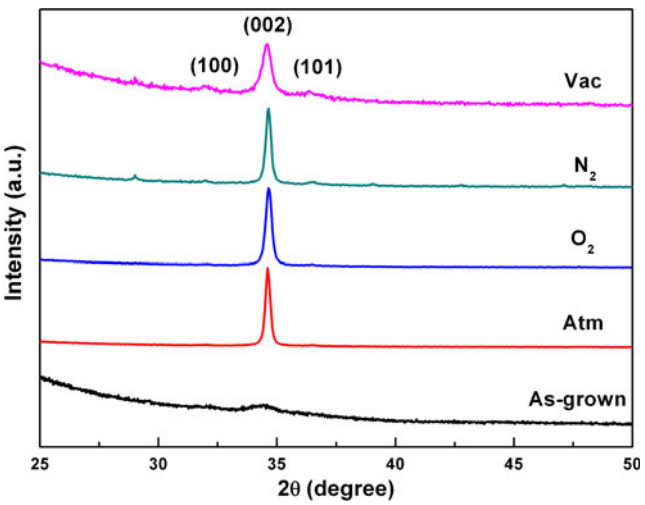


**Fig. 1** XRD patterns of ZnO thin films annealed in different ambients

**Table 1** Relative intensity of (002) orientation $\alpha_{(002)}$ values of annealed ZnO films

| | atm | $O_2$ | $N_2$ | Vacuum |
|---|---|---|---|---|
| $\alpha_{(002)}$ (%) | 97.9% | 97.8% | 93.9% | 87.5% |

size with the scherrer's formula: $D=0.94\lambda/\beta\cos\theta$, where $\lambda$, $\theta$ and $\beta$ were the X-ray wavelength, Bragg diffraction angle and FWHM in radians, respectively. Figure 2 plots the crystallite sizes of ZnO thin films against the annealing ambients. The crystalline sizes of ZnO thin films annealed in air atmosphere, $N_2$, $O_2$ and vacuum were about 44.1, 35.3, 29.4 and 25.3 nm, respectively.

Figure 3(a)–(d) show the SEM images of ZnO thin films annealed in air atmosphere, $N_2$, $O_2$ and vacuum, respectively. The surface with different features could be observed. The crystalline sizes observed in SEM were consistent with that calculated by scherrer's formula. From the figure we can see that ZnO film annealed in vacuum had the minimum grain size and some micro pores appeared on the surface. This implied that growth pressure had dominant effect on structure and surface morphology of ZnO thin films. According to Lin et al.'s research, the concentration of Zn interstitial and O vacancy is proportional with $(P_{O_2})^{-\frac{1}{2}}$ [15]. Thus more defects ought to be formed in lower growth pressure when annealing in vacuum. These defects could act as centers of nucleation and lead to more small grains. However, it is noticed that the grain size of ZnO annealed in $O_2$ is intermediate (29.4 nm). The reason may be the production of O intersititial by excess O during annealing, which pinned the grain boundary and restrained the growth of the grain.

The resistivity of ZnO thin films annealed in different ambients is shown in Fig. 4. The resistivity of ZnO thin film annealed in vacuum was 0.095 Ω·cm, which was the minimum among the four different ambients. This decrease in resistivity might be due to the increase of severe oxygen vacancies which act as the pass way of the current. However, the resistivity increased with a further increase in the oxygen concentration. The resistivity of ZnO thin films annealed in $O_2$ had the maximum value of about 129.7 Ω·cm. This increase could be explained by the decrease of oxygen vacancies because more oxygen was absorbed during annealing in abundant oxygen environment.

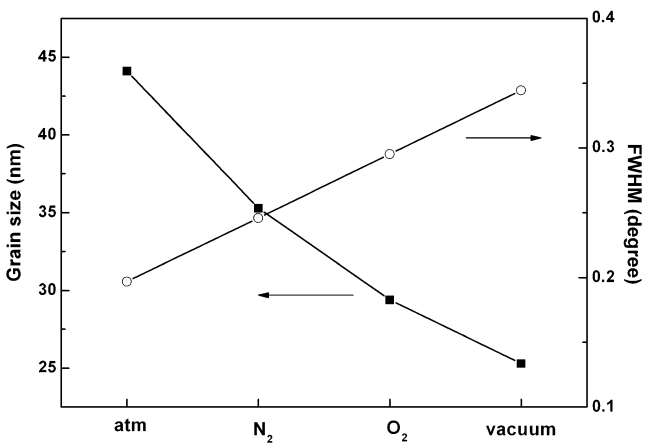


**Fig. 2** Crystalline sizes of ZnO thin films annealed in different ambients

Various structural and electrical properties will lead to various applications. For transparent electrode, it need a high transparency and low resistivity. ZnO thin film annealed in vacuum is suitable for this application. As far as TFT semiconducting channel, the major challenges is to low down the carrier concentration in the channel layer to lead to a depletion mode TFT devices. As it is known, the film porosity and grain size are connected directly with area of active surface of gas sensor, ZnO films annealed in low oxygen pressure can satisfy this demand.

The Hall Effect measurement was conducted at room temperature using the Van der Pauw method to determine the concentration and the type of the carriers. The plot of variation of carrier concentration and mobility with annealing ambients for the ZnO films annealed in air atmosphere, nitrogen, $O_2$ and vacuum are shown in Fig. 5. The ZnO thin films had the maximum carrier concentration in air atmosphere and the minimum value in $O_2$. The mobility of ZnO thin film annealed in vacuum was 105.1 $cm^2/v{\cdot}s$, which was the maximum among the four ambients. It had been known that various scattering mechanisms might be involved in semiconductor materials, including ionized impurity scattering, neutral impurity scattering, and grain-boundary scattering [16]. Though the crystallite size reduced from 44.1 to 25.3 nm after annealed in different ambients, it was still several times larger than the mean free path length, indicating the impurity scattering or other scattering centers inside the crystallite affected the film conductivity more than that of grain boundary scattering.

The carrier concentration is correlate with two parameters of the thin films, one is oxygen pressure the other is grain size. As elaborated before, low oxygen pressure will produce more Zn interstitial and O vacancy, leading to an increase of carrier concentration. On the other hand, the grain size of the film will influence the carrier concentration as well. Absorbed oxygen in grain boundaries can act as trap states, causing a decrease in carrier concentration. Thin films with small grain size will have more grain boundaries and a decrease of carrier concentration. Since we can see from the SEM images that the grain size of the ZnO film annealed in air (44.1 nm) is much larger than that annealed in vacuum (25.3 nm). We can deduce that ZnO film annealed in air will have larger carrier concentration. The

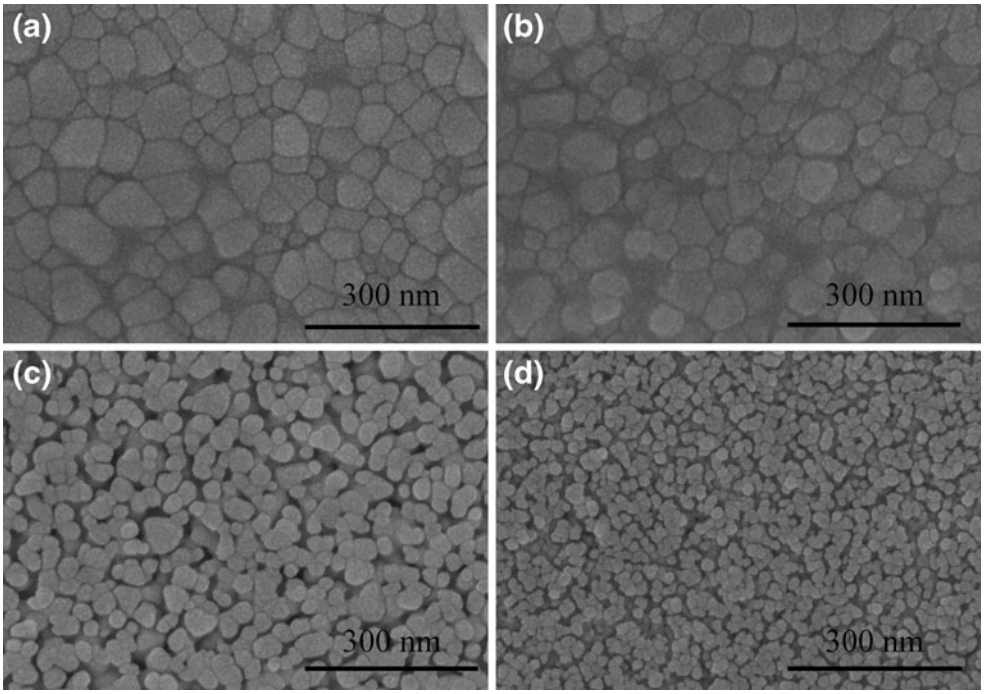


**Fig. 3** FE-SEM images of ZnO thin films annealed in different ambients (**a**) atm; (**b**) $N_2$; (**c**) $O_2$; (**d**) vacuum

carrier concentration in film is the comprehensive result of these two factors.

In order to understand the difference of the electrical properties of the ZnO films annealed in various ambients, we measured the X-ray photoelectron spectroscopy of the ZnO surface annealed in $O_2$ and vacuum, respectively. Zn 2p spectra of ZnO annealed in $O_2$ and vacuum are shown in Fig. 6(a) and (c). The binding energies were calibrated by taking carbon C 1 s peak (284.6 eV) as reference. It indicated that Zn in the films was in $2^+$ chemical states as the binding energy position of the spectra was closely matching with the standard data of zinc oxide.

XPS spectra of O 1 s of ZnO annealed in $O_2$ and vacuum are shown in Fig. 6(b) and (d). As reported in the literature that the O 1 s peak could be fitted into three peaks. The lower binding energy (~530.0±0.2 eV) corresponding to the $O^{2-}$ ions in wurtzite structure of ZnO. The higher binding energy component (~532.0±0.2 eV) was usually attributed to the presence of loosely bound oxygen species on the surface of the films, belonging to a specific species, e.g., $-CO_3$, adsorbed $H_2O$ or adsorbed $O_2$. The medium binding energy (~531.0±0.2 eV) component was associated with $O^{2-}$ ions in oxygen deficient regions within the matrix of ZnO [17, 18]. The presence as well as the changes in the intensity of this component may be related in part to the variations in the concentration of oxygen vacancies. From the XPS measurements we can see that the relative intensity ratio of medium component to total O 1 s of ZnO annealed in vacuum was much larger than that annealed in $O_2$, which indicated more deficiency in the ZnO surface when annealed in vacuum.

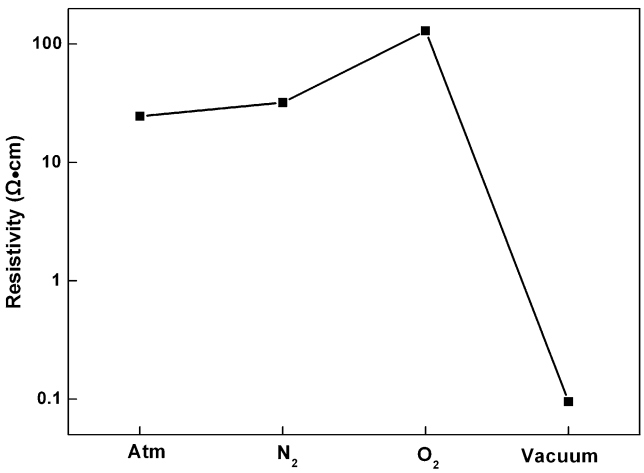


**Fig. 4** Resistivity of ZnO thin films annealed in different ambients

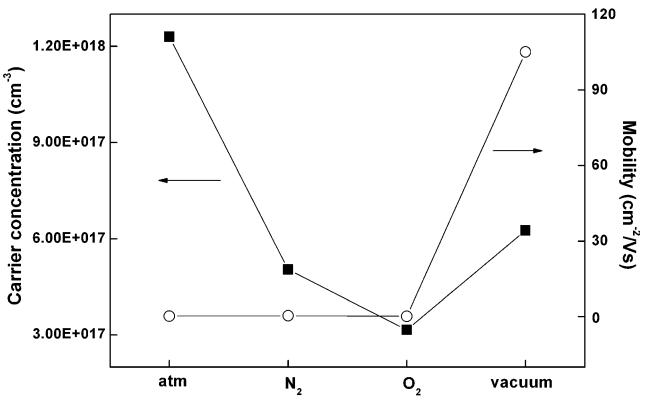


**Fig. 5** Carrier concentration and mobility of ZnO thin films annealed in different ambients

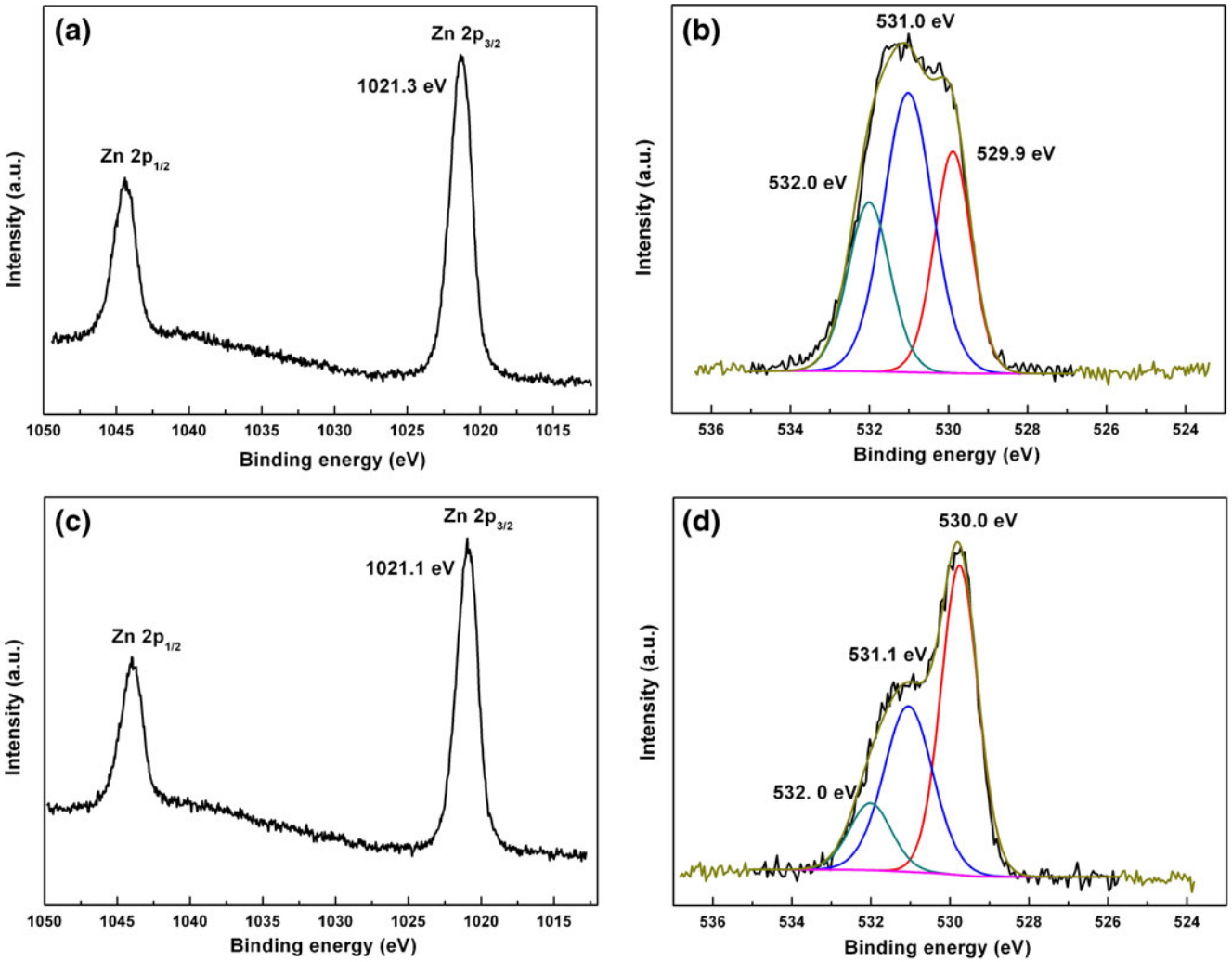


**Fig. 6** XPS spectra of the (**a**) Zn 2p region; (**b**) O 1 s region of ZnO annealed in vacuum; (**c**) Zn 2p region; (**d**) O 1 s region of ZnO annealed in $O_2$

The atomic concentration ratios of Zn to O were computed from the measured peak area together with the following sensitivity factors: Zn: 3.726; O: 0.78. The ratio of Zn to O for ZnO film annealed in $O_2$ was 1.12, and increased to 1.58 after annealed in vacuum. This implied that oxygen atoms were pumped out easily and rich zinc thin film was formed by annealing in vacuum, which lead to more zinc interstitial atoms existed within the crystal structure of ZnO films. Therefore, the defects of zinc interstitial and oxygen vacancies helped to increase electronic transition and resulted in high carrier mobility in ZnO film annealed in vacuum.

Figure 7 shows the optical transmittance spectra in the wavelength range 200–1,000 nm for ZnO thin films annealed in air atmosphere, nitrogen, $O_2$ and vacuum. The transmittance value of the blank quartz substrate was eliminated for each sample. The average optical transmittance values of ZnO thin films annealed in air atmosphere, $N_2$, $O_2$ and vacuum were about 83.5%, 80%, 82.6% and 86.2% in

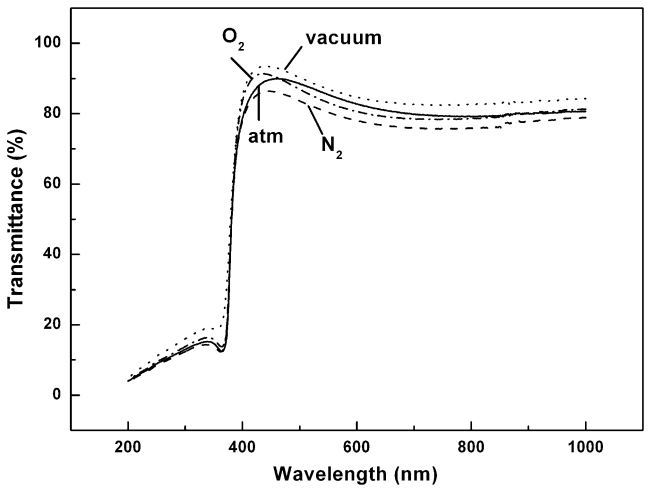


**Fig. 7** Optical transmittance spectra of ZnO thin films annealed in different ambients

the visible range (400–800 nm), respectively. Sharp absorption edges were observed in the ultraviolet region for all samples. The sharp absorption edges occurred at the wavelength of about 379 nm, which corresponding to a band gap of about 3.27 eV. This indicated that annealing ambients did not change the band gap value of ZnO thin films.

The transmittance of the film can be calculated from absorption coefficient using the relation given by Lambert-Beer's law:

$$T = \exp(-\alpha d) \quad (1)$$

where $\alpha$ is the absorption coefficient and $d$ is the thickness of the sample. $\alpha$ is found to correlate with carrier concentration (N) and mobility ($\mu$). absorption coefficient can be calculated using the following equation:

$$\alpha = c\lambda^2 N/\mu \quad (2)$$

where c is a constant value and $\lambda$ is the wavelength of the sunlight. From Fig. 5 we can see that the mobility value of ZnO film annealed in vacuum was the largest, leading to a lowest absorption coefficient value. From the Eq. 1 we can deduce that a small absorption coefficient value correlates with a high transmittence. That may be the reason why the film annealed in vacuum had the highest transmittance.

## 4 Conclusions

In summary, ZnO films deposited on quartz substrate using sol-gel technique were annealed in air atmosphere, nitrogen, $O_2$ and vacuum, respectively. Different annealing ambient had important impact on structure and electrical properties. All the annealed films were highly c-axis oriented except the film annealed in vacuum. ZnO thin film annealed in vacuum had the minimum resistivity of 0.095 Ω·cm and maximum carrier mobility of 105.1 $cm^2/v{\cdot}s$. XPS results indicated that more defects existed in the ZnO surface when annealed in vacuum than that in $O_2$. The annealed films were highly transparent with an average transmittance value exceeding 80% in the wavelength region of 400–800 nm. Various structural and electrical properties of ZnO thin films got by annealing in different ambient will have various potential application.

**Acknowledgment** This work was supported by the "Hundred Talents Program," the Chinese Academy of Sciences, the Zhejiang Natural Science Foundation (Y407364), and the Ningbo Natural Science Foundation (No. 2007A610027, No. 2008A610047, No. 2009A610018). The authors would give thanks to the all measurers of XRD, SEM, XPS and UV-Vis absorption spectroscopy of Ningbo institute of material technology & engineering Chinese academy of Science.

## References

1. S.A.M. Lima, M.R. Davolos, W.G. Quirino, C. Legnani, M. Cremona, Appl. Phys. Lett. **90**, 023503 (2007)
2. C.R. Kim, J.Y. Lee, C.M. Shin, J.Y. Leem, H. Ryu, J.H. Chang, H. C. Lee, C.S. Son, W.J. Lee, W.G. Jung, S.T. Tan, J.L. Zhao, X.W. Sun, Solid State Commun. **148**, 395 (2008)
3. B.Y. Oh, M.C. Jeong, T.H. Moon, W. Lee, J.M. Myoung, J.Y. Hwang, D.S. Seo, J. Appl. Phys. **99**, 124505 (2006)
4. P. Sagar, P.K. Shishodia, R.M. Mehra, Appl. Surf. Sci. **253**, 5419 (2007)
5. D.S. Liu, C.S. Sheu, C.T. Lee, J. Appl. Phys. **102**, 033516 (2007)
6. V.R. Shinde, T.P. Gujar, C.D. Lokhande, Sol. Energy Mater. Sol. Cells **91**, 1055 (2007)
7. C.C. Chen, B.H. Yu, J.F. Liu, Q.R. Dai, Y.F. Zhu, Mater. Lett. **61**, 2961 (2007)
8. H.Y. Tsai, J. Mater. Process. Technol. **192**, 55 (2007)
9. R. Ghosh, G.K. Paul, D. Basak, Mater. Res. Bull. **40**, 1905 (2005)
10. K.M. Lin, Y.Y. Chen, J. Sol-Gel Sci. Technol. **51**, 215 (2009)
11. S.Y. Hu, Y.C. Lee, J.W. Lee, J.C. Huang, J.L. Shen, W. Water, Appl. Surf. Sci. **254**, 1578 (2008)
12. Y.C. Lee, S.Y. Hu, W. Water, K.K. Tiong, Z.C. Feng, Y.T. Chen, J. C. Huang, J.W. Lee, C.C. Huang, J.L. Shen, M.H. Cheng, J. Lumin. **129**, 148 (2009)
13. X.Q. Wei, B.Y. Man, M. Liu, C.S. Xue, H.Z. Zhuang, C. Yang, Phys. B **388**, 145 (2007)
14. K.M. Lin, P. Tsai, Thin Solid Films **515**, 8601 (2007)
15. B.X. Lin, Z.X. Fu, Y.B. Jia, Appl. Phys. Lett. **79**, 943 (2001)
16. C. Li, M. Furuta, T. Matsuda, T. Hiramatsu, H. Furuta, T. Hirao, Thin Solid Films **517**, 3265 (2009)
17. M. Chen, X. Wang, Y.H. Yu, Z.L. Pei, X.D. Bai, C. Sun, R.F. Huang, L.S. Wen, Appl. Surf. Sci. **158**, 134 (2000)
18. X.J. Yang, X.Y. Miao, X.L. Xu, C.M. Xu, J. Xu, H.T. Liu, Opt. Mater. **27**, 1602 (2005)